Applied Science, Computing and Energy, 2026, 4(3), 407-428

Kinetic Behavior and Rate-Controlling Mechanisms Governing the Simultaneous Sequestration of Polycyclic Aromatic Hydrocarbons (PAHs) and Heavy Metals in Contaminated Soil Using Bone Biochar over Extended Contact Time

Emmanuel O. Okorodudu, Kenneth A. Ibe, Ivwurie Wisdom and Bamidele H. Akpeji
Received: 24 February 2026/Accepted: 28 April 2026/Published: 10 May 2026

Abstract: *The introduction of crude oil into soil causes the toxic, persistent, and bio-accumulative polycyclic aromatic hydrocarbons (PAHs) and heavy metals to be present in the soil, raising serious environmental and health concerns. The kinetic behaviour and rate-controlling mechanisms in sequestration of PAHs and selected heavy metals in crude oil contaminated soil with the application of bone biochar in a long contact time were investigated. Sixteen priority PAHs and selected metals (cadmium (Cd), chromium (Cr), nickel (Ni), and lead (Pb)) were monitored throughout the remediation process, including at 21, 42, 63, 84, and 105 days. The results indicated progressive reduction of the contaminants with time of contact, which suggested that the sequestration was better as the time of contact with the bone biochar increased. After 105 days, the total PAHs were reduced from 47.11 mg/kg in the untreated soil to 3.83 mg/kg, which corresponds to a removal efficiency of 91.87%. Significant reductions were also observed for Cd (75.14%), Cr (76.05%), Ni (93.38%), and Pb (89.88%). Kinetic studies confirmed that the pseudo-second-order model fits well in the adsorption process for all the contaminants, with high correlation coefficients for total PAHs (R^2 = 0.9950), Ni (R^2 = 0.9970) and Pb (R^2 = 0.9876), indicating the leading role of chemisorption mechanisms. Mechanistic evaluation showed that the mechanisms of contaminant sequestration were through surface adsorption, intraparticle diffusion, pore filling, ion exchange, electrostatic attraction, surface complexation, and mineral precipitation. The porous structure and mineral content of the biochar had a positive effect on the stabilization of contaminants in the biochar matrix. The adsorption process exhibited a multi-stage behavior: a fast initial adsorption layer, a slower diffusion-controlled adsorption and then stabilization at equilibrium. This study demonstrates that bone biochar is an efficient, sustainable, and low-cost material for soil remediation of PAHs in combination with heavy metals (HMs) for long-term use.*

Keywords: *Bone biochar, Polycyclic aromatic hydrocarbons (PAHs), Heavy metal sequestration, Adsorption kinetics, Contaminated soil remediation*

Emmanuel O. Okorodudu
Department of Industrial Chemistry, Dennis Osadebay University, Asaba, Delta State, Nigeria
Email: emmanuel.okorodudu@dou.edu.ng
https://orcid.org/0000-0002-4447-7383

Kenneth A. Ibe
Department of Chemistry, Federal University of Petroleum Resources, Effurun, Delta State, Nigeria
Email: Ibe.Kenneth@fupre.edu.ng
https://orcid.org/0000-0002-3121-7574

Ivwurie Wisdom
Department of Chemistry, Federal University of Petroleum Resources, Effurun, Delta State, Nigeria
Email: wivwurie@yahoo.co.uk
https://orcid.org/0000-0001-7026-2805

Bamidele H. Akpeji
Department of Science Laboratory Technology, Federal University of Petroleum

Resources, Effurun, Delta State, Nigeria
Email: akpeji.honesty@fupre.edu.ng
https://orcid.org/0000-0002-8404-6465

1.0 Introduction

Soil contamination by mixed organic and inorganic pollutants has become a major environmental concern worldwide, particularly in regions affected by petroleum exploration, industrial discharges, accidental oil spills, mining activities, and intensive fossil fuel combustion. Among the most hazardous contaminants frequently detected in polluted soils are polycyclic aromatic hydrocarbons (PAHs) and heavy metals (HMs) due to their persistence, toxicity, mutagenicity, carcinogenicity, and bioaccumulative characteristics. PAHs are hydrophobic organic compounds generated primarily from incomplete combustion processes and petroleum-related activities, whereas heavy metals such as cadmium (Cd), chromium (Cr), nickel (Ni), and lead (Pb) are non-biodegradable pollutants capable of persisting in environmental matrices for extended periods (Nazir *et al*., 2025). The simultaneous occurrence of PAHs and heavy metals in contaminated soils presents a serious ecological and public health challenge because both groups of contaminants may interact synergistically, thereby increasing toxicity and complicating remediation processes. Prolonged exposure to these pollutants has been associated with soil degradation, groundwater contamination, food chain transfer, mutagenicity, carcinogenicity, and several adverse human health effects.

Conventional remediation technologies for contaminated soils, including chemical oxidation, soil washing, vitrification, excavation, membrane separation, and thermal desorption, are often associated with high operational costs, secondary pollution, energy demand, and limited field applicability. Consequently, adsorption-based remediation technologies have attracted increasing attention because of their simplicity, effectiveness, low cost, and environmental sustainability. Among the different adsorbent materials investigated, biochar has emerged as one of the most promising materials for environmental remediation owing to its porous structure, high specific surface area, aromatic carbon framework, tunable surface chemistry, mineral constituents, and abundance of oxygen-containing functional groups (Zhang *et al*., 2026; Dong *et al*., 2026). Biochar is a carbon-rich material produced through the thermochemical conversion of biomass under oxygen-limited conditions and has been widely applied for the sequestration of both organic and inorganic contaminants in soil and water systems.

Recent studies have demonstrated that biochar possesses excellent adsorption potential for a broad range of pollutants, including PAHs, petroleum hydrocarbons, pesticides, dyes, endocrine-disrupting chemicals, pharmaceuticals, and heavy metals (Li *et al*., 2026; Gao *et al*., 2026). The adsorption mechanisms responsible for organic pollutant sequestration by biochar include π–π electron donor–acceptor interactions, hydrophobic partitioning, pore filling, hydrogen bonding, and electrostatic attraction, whereas heavy metal immobilization occurs mainly through ion exchange, electrostatic attraction, surface complexation, cation–π interactions, precipitation, and redox reactions (Zhang *et al*., 2026; Dong *et al*., 2026). Furthermore, the physicochemical properties of biochar, including surface area, pore volume, aromaticity, ash content, mineral composition, and functional groups, strongly influence its adsorption performance (Mogashane *et al*., 2026). Variations in feedstock type, pyrolysis temperature, residence time, and post-modification strategies also significantly determine adsorption efficiency and long-term

stability of contaminants within the biochar matrix (Li *et al*., 2026).

Bone biochar has attracted considerable attention among different biochar materials because of its unique physicochemical composition. In addition to its carbonaceous porous structure, bone biochar contains high concentrations of calcium phosphate minerals, particularly hydroxyapatite, which provide abundant active sites for heavy metal immobilization through precipitation and complexation reactions. The coexistence of carbon-rich aromatic structures and mineral phases enables bone biochar to simultaneously adsorb organic pollutants and stabilize heavy metals within contaminated soils. Studies have shown that bone biochar exhibits high adsorption capacities for both PAHs and heavy metals, making it a multifunctional remediation material for co-contaminated environments (Okorodudu *et al*., 2026). Similarly, Laishram *et al*. (2025) reported that biochar materials can achieve removal efficiencies greater than 90% for some heavy metals and more than 85% adsorption performance for various organic contaminants due to their highly tunable physicochemical properties. In addition, Onmonya *et al*. (2022) emphasized that biochar-based adsorption systems represent economical and sustainable alternatives to commercial activated carbon for heavy metal remediation.

The growing interest in biochar-based remediation has resulted in extensive investigations into adsorption mechanisms, modification strategies, and environmental applications. Mogashane *et al*. (2026) reviewed the application of biochar for PAH remediation in contaminated soils and reported that research in this area remains relatively limited despite increasing global concerns over petroleum-related contamination. Their bibliometric analysis revealed the need for additional studies focusing on mechanistic understanding, long-term stability, and large-scale implementation of biochar technologies. Similarly, Nazir *et al*. (2025) highlighted the effectiveness of biochar in reducing the bioavailability of PAHs and heavy metals at the soil–plant interface through adsorption, precipitation, and complexation processes. However, the authors identified significant uncertainties regarding contaminant remobilization, long-term performance, and ecological impacts following prolonged biochar application. Dong *et al*. (2026) further noted that biochar aging, environmental variability, and changes in soil properties may influence contaminant stability and adsorption performance over time.

Although several studies have investigated the equilibrium adsorption characteristics of biochar for pollutant remediation, most existing studies have primarily focused on adsorption isotherms and short-term remediation performance. For example, Okorodudu *et al*. (2026) evaluated the isotherm behavior and dosage-dependent performance of bone biochar for the simultaneous removal of PAHs and heavy metals over a 21-day remediation period. The study demonstrated high removal efficiencies and identified Langmuir and Freundlich isotherms as the dominant equilibrium models for different contaminants. However, the work provided limited information regarding the kinetic behavior, adsorption rates, diffusion mechanisms, and long-term sequestration processes governing contaminant removal. Similar limitations have been reported in other biochar remediation studies, where adsorption mechanisms are frequently interpreted based mainly on equilibrium conditions without detailed investigation of time-dependent adsorption dynamics (Li *et al*., 2026; Mogashane *et al*., 2026).

Kinetic investigations are essential for understanding adsorption mechanisms, predicting contaminant transport behavior, identifying rate-limiting steps, and optimizing

remediation systems for practical field applications. Common kinetic models such as pseudo-first-order and pseudo-second-order models are widely used to evaluate adsorption rates and adsorption mechanisms, while intraparticle diffusion models help identify diffusion-controlled processes involving film diffusion, pore diffusion, and surface adsorption. In co-contaminated systems, kinetic analysis becomes more complex because PAHs and heavy metals may compete for adsorption sites or interact differently with biochar surfaces depending on their physicochemical properties. Furthermore, adsorption in contaminated soils generally occurs through multi-stage processes involving rapid surface adsorption followed by slower intraparticle diffusion and eventual stabilization at equilibrium. Long-term kinetic evaluations are therefore necessary to accurately understand contaminant sequestration behavior under realistic environmental conditions.

Despite the increasing interest in biochar-based remediation technologies, there remains a significant knowledge gap regarding the long-term kinetic behavior and rate-controlling mechanisms governing the simultaneous sequestration of PAHs and heavy metals in contaminated soils using bone biochar. Most previous studies have focused mainly on equilibrium adsorption, short contact times, or single-contaminant systems, while limited information is available on the adsorption kinetics, diffusion mechanisms, and temporal sequestration behavior of mixed contaminants over extended remediation periods. In addition, the comparative kinetic responses of organic and inorganic contaminants within the same remediation system remain insufficiently understood. Addressing these gaps is essential for improving mechanistic understanding, predicting long-term remediation performance, and supporting the field-scale application of biochar technologies. Therefore, this study investigates the kinetic behavior and rate-controlling mechanisms governing the simultaneous sequestration of PAHs and selected heavy metals in crude oil–contaminated soil using bone biochar over an extended contact period of 105 days. The specific objectives are to evaluate the temporal variation in contaminant concentrations, determine the adsorption efficiencies of bone biochar over time, apply kinetic models to describe adsorption behavior, identify dominant rate-controlling mechanisms, and compare the kinetic responses of PAHs and heavy metals within the same remediation system. The findings from this study are expected to provide important insights into the long-term adsorption behavior and stabilization mechanisms of bone biochar, while contributing to the development of sustainable, low-cost, and efficient remediation technologies for petroleum-contaminated soils.

2.0 Materials and Methods

2.1 Sample Collection and Preparation

Bovine bones were collected from a public abattoir after manual removal of adhering flesh and fatty materials. The samples were transported to the laboratory in clean polyethylene bags, washed repeatedly with hot water to remove residual impurities, and oven-dried at 105 °C for 24 h. The dried bones were ground mechanically and sieved through a 0.25 mm mesh to obtain a uniform particle size before storage in airtight containers pending pyrolysis.

2.2 Bone Biochar Production

Bone biochar was produced using a temperature-controlled muffle furnace. About 50 g of the prepared bone powder was placed in covered crucibles and pyrolyzed under oxygen-limited conditions at 400 °C with a heating rate of 10 °C min^{-1} and a residence time of 2 h. After cooling to room temperature, the resulting biochar was crushed gently,

homogenized, and stored in airtight containers for further use.

2.3 Biochar Characterization

The produced bone biochar was characterized using Scanning Electron Microscopy (SEM), Fourier Transform Infrared Spectroscopy (FTIR), and Energy Dispersive X-ray (EDX) analyses to evaluate its morphology, surface functional groups, and elemental composition.

2.3.1 Scanning Electron Microscopy (SEM)

SEM analysis was carried out by mounting biochar samples on aluminium stubs using carbon adhesive tape, followed by gold coating to enhance conductivity. The samples were examined using a field emission scanning electron microscope operated at 15–20 kV. Micrographs obtained at different magnifications were used to evaluate surface morphology, pore distribution, particle aggregation, and structural uniformity. ImageJ software was further used for qualitative pore structure assessment.

2.3.2 Fourier Transform Infrared Spectroscopy (FTIR)

The biochar samples were dried, finely ground, and analyzed using FTIR within the spectral range of 4000–400 cm^{-1}. The analysis identified major surface functional groups such as hydroxyl (–OH), carbonyl (C=O), aromatic C=C, and ether linkages, which are important active sites for adsorption of PAHs and heavy metals.

2.3.3 Energy Dispersive X-ray (EDX)

EDX analysis was conducted using the SEM-EDX system operated at 20 kV and a working distance of 10 mm. Multiple regions were scanned with a dwell time of 50 s per point. The spectra obtained provided the elemental composition and atomic percentages of major elements including C, O, Ca, and P, as well as minor elements such as Mg, Na, and K.

2.4 Experimental Design

The remediation experiment was designed to evaluate the sequestration of PAHs and heavy metals from crude oil-contaminated soil using bone biochar over 105 days. Contamination was simulated by mixing 5 mL of crude oil with 50 g of air-dried soil, followed by equilibration for 7 days. A constant dose of 6 g of bone biochar was then added to each treatment sample and thoroughly mixed. Each mixture was transferred into amber glass bottles containing 20 mL of distilled water to maintain moisture content and minimize photochemical reactions.

Six experimental setups were prepared, comprising five biochar-treated samples analyzed at 21, 42, 63, 84, and 105 days, and 4 one untreated control. The contents were mixed periodically to ensure uniform interaction between soil, contaminants, and biochar. At each sampling interval, residual concentrations of PAHs and heavy metals were determined.

2.5 Analytical Methods

PAHs in the contaminated and remediated soil samples were analyzed using Gas Chromatography–Mass Spectrometry (GC–MS) following solvent extraction. About 10 g of homogenized soil was extracted using dichloromethane/hexane (1:1, v/v) under ultrasonic agitation. The extract was filtered, concentrated using a rotary evaporator, cleaned with a silica gel column, and analyzed by GC–MS. Identification and quantification were achieved using retention times, mass spectra, and external calibration standards.

Heavy metals (Cd, Cr, Ni, and Pb) were determined after acid digestion of 2 g of dried soil using a mixture of $HClO_4$, HNO_3, and H_2SO_4 (1:2:2). The digested samples were filtered, diluted to 50 mL with deionized water, and analyzed using Atomic Absorption Spectrophotometry (AAS) with calibration against standard metal solutions.

2.6 Kinetic Modeling of PAHs and Heavy Metal Removal

Adsorption kinetics were evaluated using pseudo-first-order (PFO), pseudo-second-order (PSO), and intraparticle diffusion models to investigate the adsorption mechanism and rate-controlling steps.

The linearized pseudo-first-order model is expressed as equation 1(Eddy *et al*., 2023a)

$$log(q_e - q_t) = logq_e - \frac{k_1 t}{2.303} \quad (1)$$

where q_e and q_t are the adsorption capacities at equilibrium and time t, respectively, while k_1 is the pseudo-first-order rate constant. Also, the linear form of the pseudo-second-order model is written according to equation 2 (Kelle *et al*., 2024l Ogoko *et al*., 2023)

$$\frac{t}{q_t} = \frac{1}{k_2 q_e^2} + \frac{t}{q_e} \quad (2)$$

where k_2 represents the pseudo-second-order rate constant. The intraparticle diffusion model proposed by Weber and Morris (1963) was used to evaluate diffusion-controlled adsorption processes, which is technically represented by equation 3 (Eddy *et al*., 2023b)

$$q_t = k_{id}\sqrt{t} + C + \quad (3)$$

where k_{id} is the intraparticle diffusion constant and C represents boundary layer thickness. A linear plot passing through the origin indicates intraparticle diffusion as the sole rate-controlling mechanism, whereas deviation from the origin suggests contributions from film diffusion, surface adsorption, or chemical interactions.

3.0 Results and Discussion

3.1 Characterization of Biochar

3.1.1 Scanning Electron Microscopy (SEM)

The surface morphology and structural arrangements of the fabricated bone biochar were evaluated using scanning electron microscopy. The bone biochar micrograph presented in Fig. 1 shows smoother surfaces with fewer cavities, indicating denser mineral phases where organic carbon components have fully decomposed during the thermal treatment. This specific surface morphology suggests stronger crystallization of hydroxyapatite, which enhances both the structural rigidity and the long-term chemical resistance of the biochar matrix. Although smoother surfaces generally reduce the immediate total surface area, the remaining crystalline mineral phases provide alternative and robust sorption mechanisms when interacting with polar polycyclic aromatic hydrocarbon derivatives or heavy metal co-contaminants in aqueous systems. Similar morphological contrasts between the organic and inorganic domains of bone-derived biochar have been reported to significantly influence overall sorption kinetics and pollutant-binding heterogeneity. These dense structural characteristics are particularly advantageous for heavy metal immobilization, as the rigid mineral faces act as durable platforms for active surface deposition.

3.1.2 Fourier Transform Infrared Spectroscopy (FTIR)

In the FTIR spectrum of the bone biochar shown in Fig. 2, the exceptionally strong peaks corresponding to P–O stretching located between 1200 cm^{-1} and 1000 cm^{-1} and the distinct O–P–O bending vibrations observed between 650 cm^{-1} and 500 cm^{-1} serve as definitive fingerprints of mineral-associated phosphate groups. These chemical features are highly typical of crystalline hydroxyapatite, a phase that prominently emerges as a result of high-temperature pyrolysis which efficiently eliminates the volatile organic fractions of the raw precursor. This phosphate-rich framework is exceptionally beneficial for environmental remediation, as it enables highly efficient heavy metal removal through simultaneous pathways of dissolution–precipitation, ion exchange, and surface complexation, making it particularly effective for capturing hazardous divalent cations such as lead. Conversely, the aliphatic and aromatic carbon signals are noticeably weak in the spectrum, which indicates a very high degree of organic matter decomposition and confirms the establishment

of a stable, inorganic mineral framework. While the low intensity of these organic bands implies that direct hydrophobic partitioning might be limited compared to plant-based biochars, the remaining residual carbon phases coupled with physical trapping within the newly formed pores still allow for the successful immobilization of polycyclic aromatic hydrocarbons.

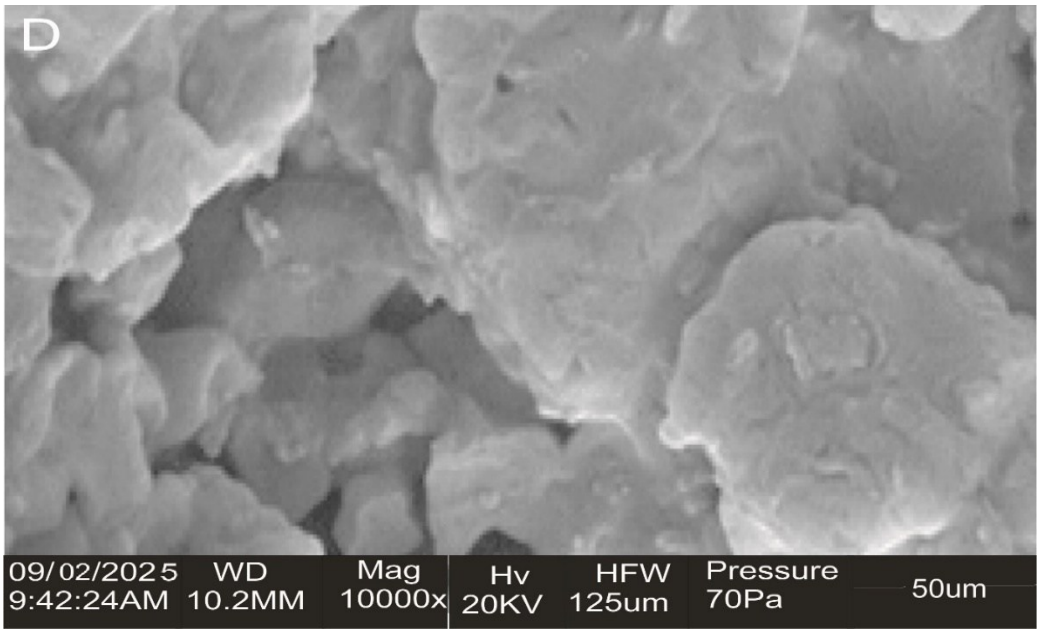

Fig. 1: Scanning Electron Microscopy (SEM) micrograph of bone biochar (BB)

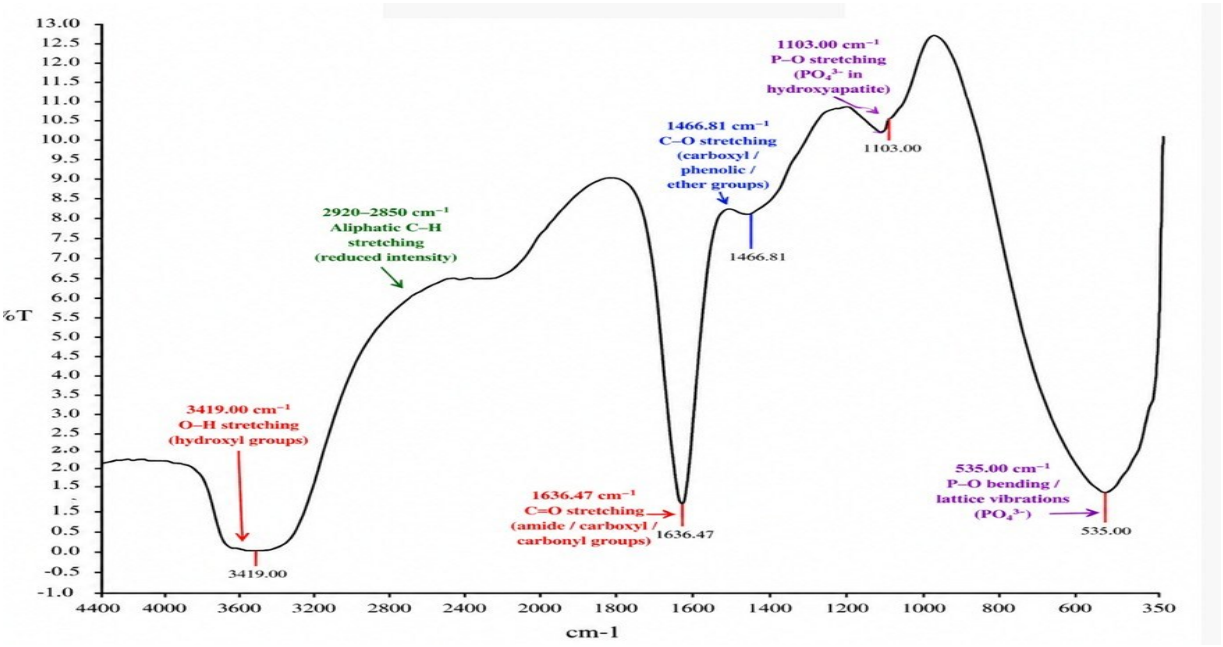

Fig. 2: FTIR spectrum of biochar obtained from bone biochar

3.1.3 Energy Dispersive X-ray Spectroscopy (EDXs)

The elemental distribution and relative weight percentages of the components making up the bone biochar were quantified using energy dispersive X-ray spectroscopy to confirm successful carbonization and mineral retention. The elemental profile displayed in Fig. 3 reveals a high accumulation of carbon at 70.26% by weight alongside a decreased oxygen content of 15.24%, which mathematically confirms a high degree of carbonization achieved during the thermal conversion process. Calcium is recorded at a significant weight concentration of 10.10%, while magnesium and iron are consistently maintained at approximately 2.00% and 2.20%, respectively, with a minor trace of silicon at 0.20%. This elevated carbon content indicates an extensive retention of fixed organic carbon and the successful formation of a carbonized bone char matrix, which represents a structural variation commonly documented in bone-derived sorbents where the exact carbon-to-calcium ratios fluctuate based on the applied heating rates and the initial biological composition of the raw bone material. The persistent and prominent presence of both calcium and iron within the samples confirms a controlled synthesis process and validates the expected mineralogical composition of the bone biochar. From an adsorption perspective, this unique elemental blend makes the material an excellent dual-purpose adsorbent. The high carbon fraction provides a hydrophobic domain suitable for binding non-polar organic molecules like polycyclic aromatic hydrocarbons via weak intermolecular forces, while the abundant calcium, iron, and magnesium components function as active, positively charged metallic sites capable of exchanging ions or forming complexes with heavy metal pollutants in contaminated media.

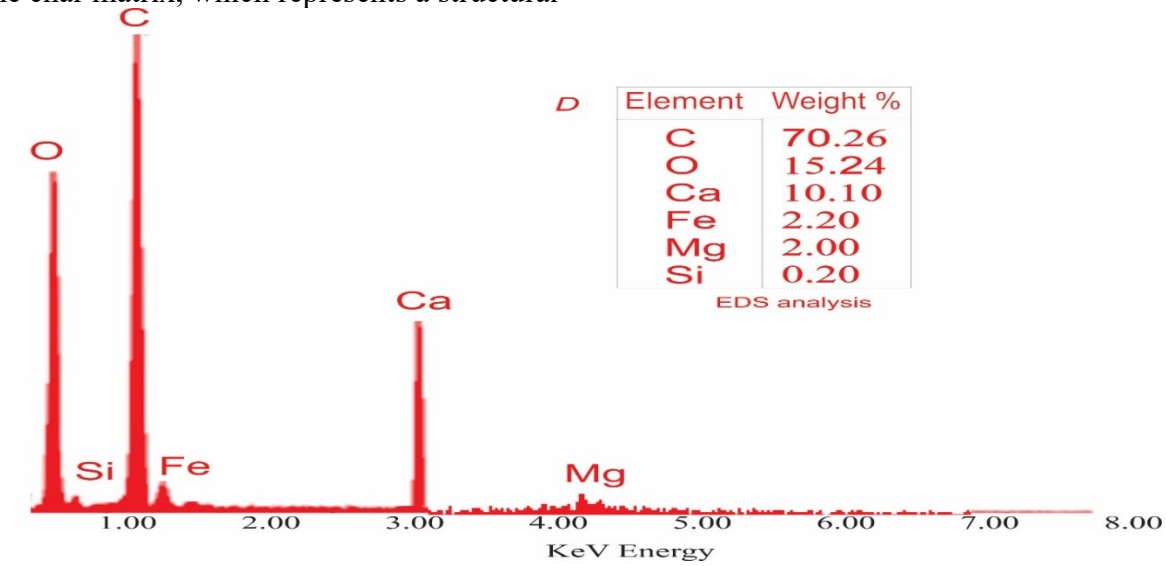

Fig. 3: EDXs spectrum of biochar obtained from bone biochar

3.2 Time-Dependent Adsorption Behavior of Bone Biochar for PAHs and Selected Heavy Metals in Crude Oil-Contaminated Soil

The multi-stage remediation profile and sequential concentration variations of the sixteen priority polycyclic aromatic hydrocarbons (PAHs) under the influence of bone biochar over an expanded operational timeframe are presented in Table 1.

Table 1: Effects of Time on Bone Biochar (BB) Sorption of PAHs of Crude Oil Contaminated Soil

S/N	16 Priority PAH Congeners	Control (soil)	BB (21 days)	BB (42 days)	BB (63 days)	BB (84 days)	BB (105 days)	% Adsorbed @ 105 days
1	Naphthalene	5.01±0.01	1.08±0.02	1.03±0.001	0.48±0.00	0.62±0.01	0.40±0.02	92.02
2	Acenaphthylene	2.56±0.00	0.55±0.04	0.52±0.01	1.45±0.00	0.32±0.03	0.20±0.00	92.19
3	Acenaphthene	5.86±0.01	1.27±0.06	1.21±0.01	2.36±0.00	0.72±0.04	0.47±0.02	91.98
4	Fluorene	3.14±0.01	0.68±0.02	0.65±0.02	0.31±0.00	0.39±0.01	0.25±0.01	92.04
5	Phenanthrene	2.03±0.01	0.50±0.01	0.48±0.02	0.06±0.00	0.25±0.01	0.18±0.00	91.13
6	Anthracene	2.44±0.01	0.65±0.02	0.62±0.01	0.59±0.00	0.45±0.02	0.25±0.00	89.75
7	Fluoranthene	1.01±0.01	0.22±0.01	0.21±0.01	0.18±0.00	0.19±0.01	0.08±0.00	92.08
8	Pyrene	1.44±0.01	0.31±0.01	0.30±0.02	0.04±0.00	0.18±0.01	0.11±0.01	92.36
9	Benz[a]anthracene	2.56±0.01	0.55±0.01	0.52±0.01	0.01±0.00	0.32±0.01	0.20±0.00	92.19
10	Chrysene	3.82±0.01	0.83±0.01	0.78±0.02	0.06±0.00	0.47±0.01	0.31±0.02	91.88
11	Benzo[b]fluoranthene	4.27±0.01	0.92±0.01	0.88±0.01	0.55±0.00	0.53±0.01	0.35±0.01	91.80
12	Benzo[k]fluoranthene	2.79±0.01	0.60±0.01	0.57±0.00	0.58±0.00	0.34±0.01	0.22±0.01	92.11
13	Benzo[a]pyrene	2.19±0.01	0.47±0.01	0.45±0.00	0.82±0.00	0.27±0.01	0.17±0.00	92.24
14	Indeno[1,2,3-cd]pyrene	2.44±0.01	0.53±0.01	0.50±0.00	0.15±0.00	0.30±0.01	0.20±0.00	91.80
15	Dibenz[a,h]anthracene	2.55±0.01	0.55±0.01	0.52±0.02	0.05±0.00	0.31±0.01	0.20±0.01	92.16
16	Benzo[ghi]perylene	3.00±0.01	0.65±0.01	0.62±0.01	0.18±0.00	0.37±0.01	0.24±0.01	92.00
	Total PAH (mg/kg)	47.11±0.15	10.36±0.21	9.86±0.18	7.87±0.00	6.03±0.22	3.83±0.12	

The untreated control soil, as visualized in the experimental trend shown in Fig. 4, recorded exceptionally high initial concentrations of organic contaminants with a combined total PAH value of 47.11 mg/kg, which confirms severe environmental contamination typical of petroleum-impacted terrestrial systems. Following the structural amendment of the soil with bone biochar, the specific concentrations of all individual PAH congeners decreased progressively and systematically across each monitored interval from day 21 to day 105. By the conclusion of the 105-day remediation cycle, the total lingering concentration of PAHs dropped significantly to 3.83 mg/kg, demonstrating a highly substantial and successful overall clean-up of the soil system. This profound reduction indicates that the synthesised bone biochar exhibits an outstanding adsorption affinity for hydrophobic organic pollutants, directly attributable to its highly porous structure, large internal surface area, and integrated mineral active sites. Animal bone-derived chars are known to efficiently immobilize dense rings of organic contaminants within complex soil matrices.

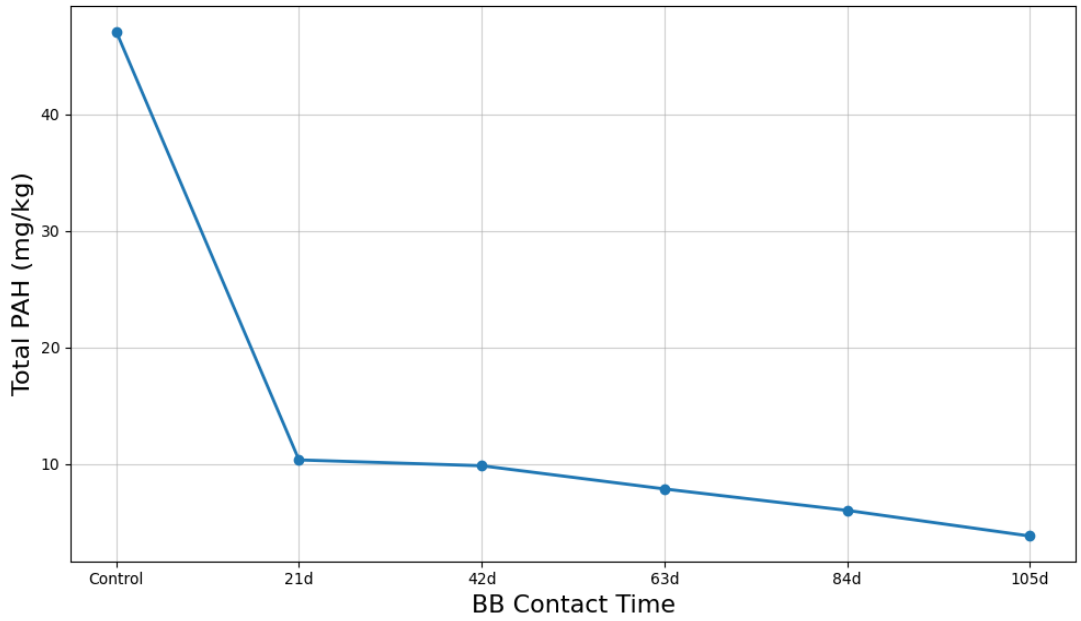

Fig. 4: Line graph of total PAH vs contact time for bone biochar

This strong downward concentration trend was immediately apparent among the low molecular weight PAHs including naphthalene, acenaphthylene, acenaphthene, and fluorene. For example, naphthalene levels dropped sharply from an initial 5.01 mg/kg in the control soil to a mere 0.40 mg/kg by day 105, which represents a calculated 92.02% adsorption efficiency, while acenaphthylene concentrations concomitantly decreased from 2.56 mg/kg to 0.20 mg/kg, equating to a 92.19% total removal. These lower-ring compounds possess higher environmental volatility and higher aqueous solubility compared to their heavier counterparts, which inherently increases their mobility and makes them more accessible to rapid surface adsorption and localized microbial degradation pathways. The carbonized surfaces of the bone biochar are rich in specialized aromatic configurations that readily facilitate the formation of tight π–π electron donor-acceptor interactions with corresponding PAH rings, allowing for highly efficient initial capture

from the soil matrix. The steady, continuous decline observed across the experimental timeline suggests that sufficient contact time is a vital parameter, allowing these lighter organic molecules to migrate deeply via pore diffusion into the deeper micro- and mesoporous cavities of the adsorbent.

Intermediate molecular weight PAHs, which are composed of three-ring and four-ring assemblies such as phenanthrene, anthracene, fluoranthene, and pyrene, also demonstrated major reductions during the remediation period. Phenanthrene concentrations decreased markedly from 2.03 mg/kg to 0.18 mg/kg, while anthracene declined from 2.44 mg/kg to 0.25 mg/kg at the 105-day mark, with fluoranthene and pyrene following a similar trajectory to reach low residuals of 0.08 mg/kg and 0.11 mg/kg, respectively. These values demonstrate that the bone biochar matrix works effectively across varying molecular dimensions. Biochars synthesized from animal waste materials combine a rigid carbonaceous core with highly reactive calcium phosphate mineral phases, which collectively maximize organic contaminant removal by pairing hydrophobic surface interactions with direct mechanical pore trapping. Furthermore, the removal trends observed for high molecular weight PAHs including benz[a]anthracene, chrysene, benzo[b]fluoranthene, and benzo[k]fluoranthene validate the broad-spectrum efficiency of this bone-derived material. Chrysene levels fell from 3.82 mg/kg in the baseline control soil to 0.31 mg/kg after 105 days, while benz[a]anthracene decreased from 2.56 mg/kg to 0.20 mg/kg. High molecular weight PAHs are notoriously difficult to eliminate due to their massive, complex condensed ring systems and low water solubility, but the high hydrophobic attraction and physical pore entrapment provided by the biochar matrix overcome these challenges, yielding the exceptionally high percentage removal values documented in Table 1.

Crucially, the highly dangerous carcinogenic PAHs, including benzo[a]pyrene, indeno[1,2,3-cd]pyrene, dibenz[a,h] anthrac - ene, and benzo[ghi]perylene, exhibited substantial and sustained decreases over the course of the treatment. The highly toxic index compound benzo[a]pyrene plummeted from 2.19 mg/kg in the control soil to 0.17 mg/kg at the end of 105 days, securing a 92.24% adsorption level, while indeno[1,2,3-cd]pyrene dropped from 2.44 mg/kg to 0.20 mg/kg. Because these specific compounds pose severe toxicological, mutagenic, and carcinogenic risks to human health and local food webs, achieving such low residual limits is a vital benchmark for verified environmental remediation. Applying these bone biochar amendments effectively mitigates these risks by reducing the bioavilability and lateral migration of these hazardous chemicals, tethering them tightly to the solid carbon surfaces. The total drop in total PAHs from 47.11 mg/kg to 3.83 mg/kg over 105 days underlines how crucial contact time is for achieving high performance, as the contaminants must migrate from the bulk soil solution into the internal pore networks via slow, rate-limiting intra-particle diffusion. Unlike standard plant-derived chars, the high concentration of crystalline hydroxyapatite and stable calcium minerals inside bone biochar provides structural support that prevents pore collapse, ensuring a steady abundance of active binding sites over extended field periods. The resulting 89% to 92% removal efficiencies show that transforming waste bone into biochar is a highly viable, sustainable, and cost-efficient strategy for the long-term clean-up of petroleum-polluted soils.

3.2.2 Effect of Contact Time on the Sorption of Selected Heavy Metals

The quantitative impact of processing time on the multi-metal immobilization performance of bone biochar within the contaminated soil

matrix is summarized in Table 2, documenting the individual concentration drops for cadmium, chromium, nickel, and lead.

The visual overview of these heavy metal concentration profiles as a function of remediation time is shown in the line graph in Fig. 5. The untreated baseline control soil contained very high levels of toxic metals, led by a massive lead accumulation of 207.42 mg/kg and a cadmium level of 72.56 mg/kg, which reflects severe heavy metal co-contamination commonly introduced during industrial petroleum exploitation. Following introduction of the bone biochar, a steady, continuous decline in all four metallic targets was noted through day 105, showing that heavy metal immobilization is enhanced with long contact periods. By day 105, cadmium concentrations fell to 18.04 mg/kg (75.14% removal) and chromium decreased to 15.13 mg/kg (76.05% removal).

This time-dependent behavior matches a multi-step mechanism where hydrated metallic ions slowly diffuse from the outer soil solution into the internal porous channels of the biochar, where they encounter active mineral surface sites. The high surface area, cation exchange capacity, and dense functional groups of the adsorbent are central to keeping these hazardous metals bound tightly to the solid phase.

Cadmium removal progressed steadily across the entire testing timeframe, declining from 72.56 mg/kg to 18.04 mg/kg. Even though its final removal efficiency of 75.14% was slightly lower than that of lead or nickel, the continuous, uniform downward trend indicates that the bone biochar successfully binds free Cd^{2+} ions. This occurs through ion exchange with native matrix cations, surface complexation, and direct electrostatic attraction. Oxygen-rich surface groups on the biochar, such as carboxyl and hydroxyl networks, form stable chemical complexes with these divalent cations, preventing them from leaching into surrounding ecosystems or being taken up by plants.

Table 2: Effects of Time on Bone Biochar (BB) Sorption of Some Selected Heavy Metals of Crude Oil Contaminated Soil

Treatment/Duration	Cd (mg/kg)	Cr (mg/kg)	Ni (mg/kg)	Pb (mg/kg)
Control (soil)	72.56 ± 0.01	63.17 ± 0.01	14.20 ± 0.01	207.42 ± 0.02
BB (21 days)	41.94 ± 0.08	30.40 ± 0.53	3.73 ± 0.35	89.50 ± 0.05
BB (42 days)	40.41 ± 0.01	28.01 ± 0.01	3.06 ± 0.01	71.03 ± 0.01
BB (63 days)	34.90 ± 0.02	24.03 ± 0.03	1.99 ± 0.02	37.18 ± 0.02
BB (84 days)	24.14 ± 0.02	22.59 ± 0.01	1.54 ± 0.01	21.59 ± 0.00
BB (105 days)	18.04 ± 0.01	15.13 ± 0.01	0.94 ± 0.01	20.99 ± 0.02
% Adsorbed @ 105 days	75.14	76.05	93.38	89.88

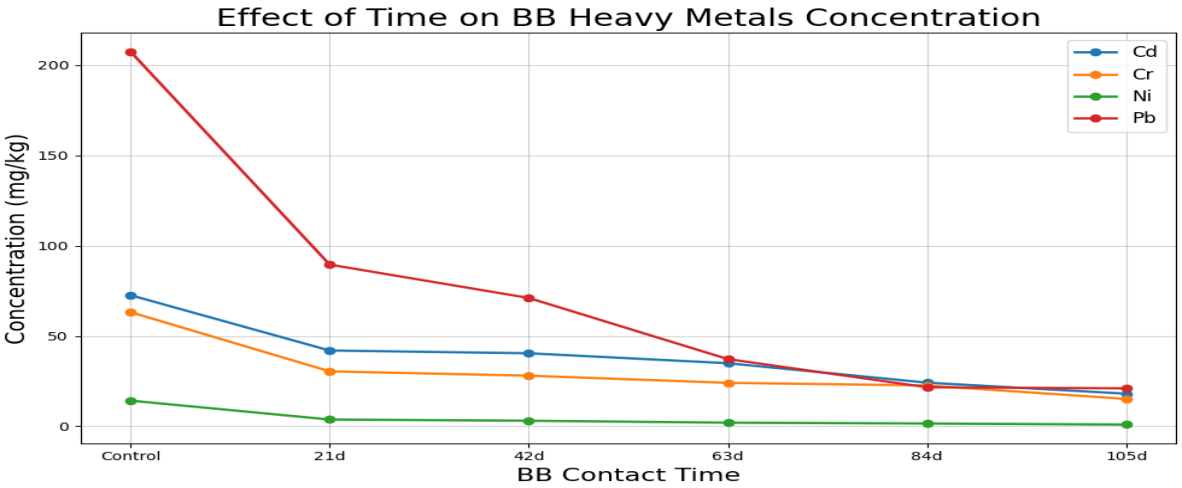

Fig. 5: Line graph of Cd, Cr, Ni, and Pb vs contact time for bone biochar

This steady immobilization mechanism matches established models for cadmium capture using premium engineered chars. Chromium also dropped considerably over time, falling from 63.17 to 15.13 mg/kg to achieve a 76.05% removal efficiency. The immobilization of chromium on bone biochar often involves several overlapping pathways, including direct surface adsorption, chemical reduction of mobile hexavalent species to less toxic trivalent states, and localized precipitation within the biochar pores. The calcium-rich hydroxyapatite mineral phases in the bone char matrix play an active role here, providing inorganic support that can trigger precipitation or co-crystallization reactions to lock chromium ions into place.

Nickel and lead concentrations showed the most dramatic declines over the 105-day remediation period. Nickel fell from 14.20 mg/kg to an extremely low 0.94 mg/kg, leading all tested metals with a 93.38% removal efficiency, while lead plunged from 207.42 mg/kg down to 20.99 mg/kg, securing an 89.88% removal. This superior performance indicates that Ni2+ and Pb2+ ions have an exceptionally high thermodynamic affinity for the specific binding sites on bone biochar, taking full advantage of the open pore structure. Additionally, the inherently alkaline nature of bone-derived biochar helps raise the local soil pH around the amendment particles. This localized pH increase promotes the formation of insoluble metal hydroxides and carbonates, causing the target heavy metals to precipitate out of solution. As a result, adding bone biochar effectively lowers the bioavailability and migration of dangerous heavy metals while helping restore overall soil stability.

3.3 Kinetic Modeling of PAHs and Heavy Metals Adsorption onto Bone Biochar

To investigate the adsorption rate and determine the underlying physical and chemical mechanisms controlling contaminant sequestration over time, pseudo-first-order (PFO) and pseudo-second-order (PSO) kinetic models were systematically applied to the experimental data.

3.3.1 Adsorption Kinetics of PAHs

The time-dependent removal of the 16 priority polycyclic aromatic hydrocarbons (PAHs) was mathematically evaluated using linear forms of both PFO and PSO frameworks. The generated PFO linear regression yielded the equation $\log(qe-qt)=-0.007578t-1.045321$, with a calculated rate constant (k1) of 0.017452 day−1 and a coefficient of determination (R2) of 0.9051. This high R2 value shows that the PFO model gives a

reasonable approximation of the system during the early stages of remediation, where the rate of contaminant uptake is primarily governed by the abundant availability of unoccupied active sites on the external surface of the biochar. This initial phase is dominated by physical adsorption pathways, including hydrophobic configurations, van der Waals forces, and boundary-layer film diffusion.

As the system approached long-term operational equilibrium, the experimental data showed superior alignment with the PSO kinetic model. The linear PSO regression yielded the equation $t/qt = 2.643739t + 20.051755$, providing a rate constant (k2) of 0.348566 g·mg−1·day−1 and a highly significant correlation coefficient (R2) of 0.9950. The superior fit of the PSO model confirms that chemisorption operates as the principal rate-limiting step over the entire 105-day cycle. This process involves valency-driven electron sharing or exchange between the condensed aromatic rings of the PAHs and the surface functional groups of the bone biochar. These chemical interactions are enhanced by the structural matrix of the biochar, which supports π−π electron donor-acceptor systems, localized hydrogen bonding, and surface complexation that firmly bind the organic molecules.

3.3.2 Adsorption Kinetics of Heavy Metals (Cd^{2+}, Cr^{n+}, Ni^{2+}, and Pb^{2+})

The kinetic profiles for the simultaneous immobilization of heavy metal co-contaminants were modeled using both PFO and PSO equations to identify changes in binding mechanisms across the different metal species. The calculated linear equations and corresponding statistical parameters for both models are presented within the text and summarized in the comprehensive master kinetic table.

For the PFO model, the linear relationships were derived by plotting log(qe−qt) against time (t). The Cd^{2+} system produced the linear equation $\log(qe-qt) = -0.009057t - 0.418615$ (k_1=0.020859 day−1; $R^2 = 0.8003$), reflecting a moderate fit that indicates physical surface diffusion occurred alongside more complex chemical processes. Chromium displayed a much tighter conformity to first-order mechanics, yielding the equation $\log(q_e-q_t) = -0.0052t - 0.776754$ with a rate constant k_1= 0.011996 day−1 and a strong correlation coefficient (R^2 = 0.9763). Similarly, nickel (Ni^{2+}) removal showed a high first-order correlation (R^2=0.9747) via the equation $\log(q_e-q_t) = -0.010988t - 1.359485$($k_1$= 0.0253 day^{-1}). Lead ion displayed the equation $\log(q_e-q_t) = -0.031728t + 0.717156$ (k_1=0.073070 day^{-1}; R^2=0.8357). The high initial rate constant for lead indicates rapid early migration and accumulation on the accessible outer surface of the biochar particle.

When the heavy metal data were fitted to the PSO framework by plotting t/qt versus t, the correlation coefficients generally improved (Fig. 6), confirming the dominant role of chemisorption in the long-term stabilization of the inorganic ions. The cadmium system followed the equation $t/q_t = 1.662051t + 71.109617$, yielding a second-order rate constant (k_2) of 0.03885 g·mg−1·day−1 and an improved R2 of 0.8806, which shows that surface complexation with oxygen-containing functional groups controls Cd^{2+} immobilization. The chromium adsorption data yielded the equation, $\frac{t}{q_{\square}} = 2.2658t + 42.0702$ ($k_2 = 0.1220\ g.mg^{-1}$, (R^2 = 0.9543), indicating that precipitation, reduction reactions, and electrostatic interactions with the hydroxyapatite mineral matrix drive chromium removal.

Nickel displayed the highest overall fit to the second-order model, generating the linear equation $t/q_t = 8.39458t + 82.8836$ with an excellent correlation coefficient (R^2 = 0.9970) and a rate constant k_2= 0.85022 $g{\cdot}mg^{-1}{\cdot}day^{-1}$. This strong fit indicates that Ni^{2+} ions form

highly stable coordinate bonds with active surface ligands. Lead remediation also showed strong conformity to the PSO model, achieving an R^2 of 0.9876. This high value confirms that Pb^{2+} is immobilized primarily through chemical pathways, including ion exchange with the calcium phases of the bone biochar and direct surface precipitation of mineral complexes.

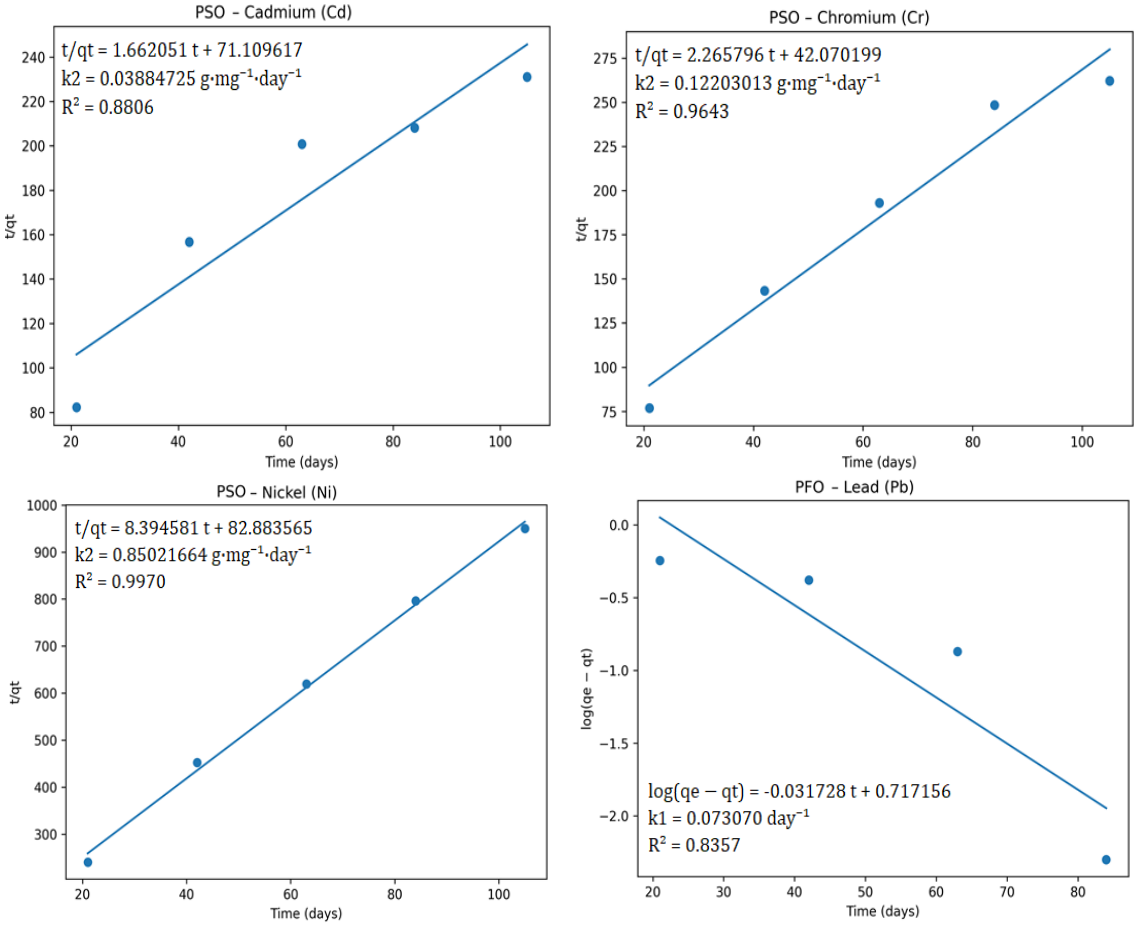

Fig. 6: Pseudo-Second-Order (PSO) modelling for Cd, Cr, Ni, and Pb adsorption

3.3.3 Intraparticle Diffusion and Multi-Stage Sequestration Mechanisms

To understand the specific diffusion pathways and mass-transport limitations regulating contaminant uptake, the experimental data were analyzed using the Weber-Morris intraparticle diffusion model. The calculated kinetic parameters, including the intraparticle diffusion rate constant (kid), the boundary layer intercept (C), and the correlation coefficients (R^2), are presented in Table 3.The intraparticle diffusion plots shown in Fig. 7 confirm that the sequestration of both organic and inorganic pollutants on bone biochar is a multi-stage process rather than a single diffusion-limited event. The plots show a distinct multi-linear profile defined by two sequential stages: a rapid initial phase representing external boundary-layer film diffusion, followed by a slower, extended linear region reflecting intraparticle pore diffusion as the system approaches equilibrium. Because none of the regression lines pass through the origin (as indicated by the positive values of the intercept C in Table

3), intraparticle pore diffusion is not the sole rate-limiting step; instead, film diffusion and active surface chemical interactions operate simultaneously throughout the process.

Table 3: Calculated Intraparticle Diffusion Parameters for PAHs and Heavy Metals

Contaminant	k_{id} (mg·g^{-1}·day$^{-1/2}$)	C	R^2	Regression Equation
Total PAHs	0.0097	0.2547	0.9171	$q_t=0.0097t_{1/2}+0.2547$
Cadmium (Cd)	0.0367	0.0570	0.8883	$q_t=0.0367t_{1/2}+0.0570$
Chromium (Cr)	0.0207	0.1669	0.8943	$q_t=0.0207t_{1/2}+0.1669$
Nickel (Ni)	0.0042	0.0672	0.9865	$q_t=0.0042t_{1/2}+0.0672$
Lead (Pb)	0.1121	0.4672	0.9474	$q_t=0.1121t_{1/2}+0.4672$

During the initial phase of remediation, the rapid decrease in contaminant levels is driven by the immediate availability of active binding sites across the external surface of the bone biochar. For the organic PAHs, this rapid uptake is mediated by hydrophobic partitioning and π–π electron interactions with the aromatic carbon core. For the heavy metal ions, this early capture is driven by strong electrostatic attraction and rapid ion exchange with negatively charged surface functional groups.
As these easily accessible external sites become saturated, the rate-limiting step shifts to the slow migration of target molecules into the internal pore structure of the biochar. The porous networks and irregular surface morphology confirmed by SEM analysis provide channels that allow Cd2+, Crn+, Ni2+, Pb2+, and condensed PAH rings to diffuse deep into the internal carbonaceous matrix. The high PSO correlation values (R2=0.9950 for total PAHs; R2≥0.9643 for Ni, Pb, and Cr) confirm that once these molecules finish migrating through the pores, they are permanently locked in place by chemisorption, surface complexation, and mineral precipitation with the hydroxyapatite component.

3.3.4 Comparative Evaluation of Kinetic Models and Equilibrium Behaviour

A comparative analysis of the PFO and PSO frameworks shows distinct differences in how effectively each model captures the long-term immobilization of organic and inorganic species on the bone biochar surface. The key parameters, best-fit selections, and primary binding mechanisms are summarized in Table 4.

Table 4: Comparative Kinetic Parameters and Dominant Adsorption Mechanisms

Contaminant	PFO R2	PSO R2	Best Fit Model	Dominant Mechanism
Total PAHs	0.9051	0.9950	PSO	Chemisorption + intraparticle pore diffusion
Cadmium (Cd)	0.8003	0.8806	PSO	Surface complexation + ion exchange
Chromium (Cr)	0.9763	0.9643	PFO / PSO	Mixed physical adsorption + chemical reduction
Nickel (Ni)	0.9747	0.9970	PSO	Coordinate chemisorption on surface sites
Lead (Pb)	0.8357	0.9876	PSO	Mineral interaction + surface precipitation

The higher correlation coefficients calculated for the PSO model across almost all tested contaminants indicate that valence-driven chemical interactions dominate long-term sequestration. The mineral-rich composition of the bone biochar—characterized by a stable framework of crystalline hydroxyapatite and active phosphate phases—enhances metal immobilization by driving surface precipitation and complexation reactions. The lower correlation coefficients for the PFO model during the later stages of cadmium and lead removal show that purely physical adsorption cannot fully account for the behavior of this system. However, the strong PFO fit observed for chromium and nickel shows that external surface diffusion remains a major factor during the initial stages of treatment before chemisorption takes over.

The multi-stage approach to equilibrium over the 105-day remediation period indicates that contaminant removal on bone biochar is a gradual, transport-mediated process rather than simple surface saturation. This slow progress toward equilibrium occurs because target molecules must migrate through the dense internal pore structure of the biochar to reach deep-seated binding sites. Total PAH adsorption increased from 78.01% at day 21 to 91.87% at day 105, demonstrating that extended contact time allows for thorough diffusion and secure chemical stabilization. This synergistic combination of film diffusion, intraparticle pore filling, ion exchange, surface complexation, and mineral precipitation confirms that bone biochar functions as an effective, multi-purpose adsorbent capable of simultaneously isolating organic and inorganic pollutants from co-contaminated soils.

4.0 Conclusion

This study demonstrated the ability of bone biochar to extract polycyclic aromatic hydrocarbons (PAHs) and certain heavy metals from crude oil contaminated soil over a long remediation period. The results indicated that the adsorption efficiency was improved gradually as the contact time between contaminants and bone biochar increased, suggesting that an extended interaction between contaminants and bone biochar promoted adsorption and stabilization in the soil matrix. After 105 days of remediation, significant reductions in contaminant concentrations were seen. The total PAHs were reduced from 47.11 mg/kg in the untreated contaminated soil to 3.83 mg/kg, which is an adsorption efficiency of 91.87%. Similarly, cadmium (Cd), chromium (Cr), nickel (Ni), and lead (Pb) recorded removal efficiencies of 75.14%, 76.05%, 93.38%, and 89.88%, respectively. The results reaffirm the high remediation capability of bone biochar to remove both organic and inorganic contaminant at the same time from contaminated soil. The pseudo second-order model was found to be the most suitable model for the majority of contaminants with the adsorption being dominated by chemisorption. Several factors such as surface adsorption, intraparticle diffusion, pore filling, ion exchange, electrostatic attraction, and surface complexation determined the adsorption behaviour. It also showed multi-stage adsorption behaviour with fast adsorption at initial stages, followed by diffusion-controlled adsorption and reaching equilibrium saturation level over time. The SEM analysis showed the porous and non-uniform surface structure of the bone biochar, promoting the diffusion and adsorption of contaminants inside the pores. The FTIR results verified the presence of functional groups which facilitate the binding and surface interactions of the contaminants, and the EDX results confirmed the presence of minerals that were responsible for the immobilization and stabilization of the heavy metals in the biochar. The findings of the study make bone biochar a potential efficient, sustainable, and low-cost adsorbent for the

cleanup of crude oil-contaminated soils. Therefore, the physical and chemical adsorption mechanisms revealed in the present study further demonstrate the applicability of bone biochar for long-term environmental remediation and contaminant management applications.

Acknowledgement

The authors gratefully acknowledge the technical assistance provided by the laboratory staff of the Department of Chemistry, Federal University of Petroleum Resources, Effurun. We also thank the staff and management of Jacio Environmental Limited for their valuable support.

5.0 References

Akbarpour, A., & Yousefi Kebria, D. (2025). Kinetic and Thermodynamic Study on Removal of PAH from Water using the Performance of Modified Natural Adsorbent. *Iranica Journal of Energy and Environment*, *16*(2), 196–204. https://doi.org/10.5829/ijee.2025.16.02.03

Azeem, M., Arockiam Jeyasundar, P. G. S., Ali, A., Riaz, L., Khan, K. S., Hussain, Q., Kareem, H. A., Abbas, F., Latif, A., Majrashi, A., Ali, E. F., Li, R., Shaheen, S. M., Li, G., Zhang, Z., & Zhu, Y.-G. (2023). Cow bone-derived biochar enhances microbial biomass and alters bacterial community composition and diversity in a smelter contaminated soil. *Environmental Research*, *216*(1), 114278. https://doi.org/10.1016/j.envres.2022.114278

Azeem, M., Shaheen, S. M., Ali, A., Jeyasundar, P. G. S. A., Latif, A., Abdelrahman, H., Li, R., Almazroui, M., Niazi, N. K., Sarmah, A. K., Li, G., Rinklebe, J., Zhu, Y.-G., & Zhang, Z. (2022). Removal of potentially toxic elements from contaminated soil and water using bone char compared to plant- and bone-derived biochars: A review. *Journal of Hazardous Materials*, *427*, 128131. https://doi.org/10.1016/j.jhazmat.2021.128131

Ding, Y., Zhu, S., Pan, R., Bu, J., Liu, Y., & Ding, A. (2022). Effects of Rice Husk Biochar on Nitrogen Leaching from Vegetable Soils by 15N Tracing Approach. *Water*, *14*(21), 3563–3563. https://doi.org/10.3390/w14213563

Eddy, N. O., Odiongenyi, A. O., Garg, R., Ukpe, R. A., Garg, R., El Nemir, A., Ngwu, C. M.& Okop, I. J. (2023a). Quantum and experimental investigation of the application of *Crassostrea gasar* (mangrove oyster) shell–based CaO nanoparticles as adsorbent and photocatalyst for the removal of procaine penicillin from aqueous solution. *Environmental Science and Pollution Research*, doi:10.1007/s11356-023-26868-8

Eddy, N. O., Garg, R., Garg, R., Ukpe, R. A., & Abugu, H. (2023b). Adsorption and photodegradation of organic contaminants by silver nanoparticles: Isotherms, kinetics, and computational analysis. *Environmental Monitoring and Assessment*. https://doi.org/10.1007/s10661-023-12194-6

Eddy, N. O., Garg, R., Garg, R., Ukpe, R. A. & Abugu, H. (2023b). Adsorption and photodegradation of organic contaminants by silver nanoparticles: isotherms, kinetics, and computational analysis. *Environmental Monitoring and Assessment*,, doi: : 10.1007/s10661-023-12194-6,

Ezzati, R. (2020). Derivation of Pseudo-First-Order, Pseudo-Second-Order and Modified Pseudo-First-Order rate equations from Langmuir and Freundlich isotherms for adsorption. *Chemical Engineering Journal*, *392*, 123705. https://doi.org/10.1016/j.cej.2019.123705

Ghaedi, S., Rajabi, H., Hadi Mosleh, M., & Sedighi, M. (2024). MOF biochar composites for environmental protection and pollution control. *Bioresource Technology*, *418*, Article 131982.

https://doi.org/10.1016/j.biortech.2024.131982

Ghorbani, M., Azarnejad, N., Brown, R. W., Chadwick, D. R., Loppi, S., & Jones, D. L. (2026). Sustainable resource management with bone char-challenges and opportunities for enhancing soil health and phosphorus stocks. *Biochar*, *8*, Article 34. https://doi.org/10.1007/s42773-025-00550-3

Gong, H., Zhao, L., Rui, X., Hu, J., & Zhu, N. (2022). A review of pristine and modified biochar immobilizing typical heavy metals in soil: Applications and challenges. *Journal of Hazardous Materials*, 432, 128668. https://doi.org/10.1016/j.jhazmat.2022.128668

Kelle, H. I., Ogoko, E. C., Akintola O & Eddy, N. O. (2023). Quantum and experimental studies on the adsorption efficiency of oyster shell–based CaO nanoparticles (CaONPO) towards the removal of methylene blue dye (MBD) from aqueous solution. *Biomass Conversion and Biorefinery, 14*, 31925–31948. https://doi.org/10.1007/s13399-023-04947-7.

Karthik, V., Periyasamy, S., Dharneesh, S., Duvakeesh, G. K., Gizaw, D. G., & Vijayashankar, T. (2024). Biochar as a sustainable adsorbent for heavy metal removal from polluted waters: A comprehensive outlook. *Journal of Chemistry, 2024, 8217730.* https://doi.org/10.1155/joch/8217730

Khurshid, H., Mustafa, M. R. U., Isa, M. H., & Mignardi, S. (2022). A comprehensive insight on adsorption of polyaromatic hydrocarbons, chemical oxygen demand, pharmaceuticals, and chemical dyes in wastewaters using biowaste carbonaceous adsorbents. *Bioinorganic Chemistry and Applications*, *2022*, 2022. https://doi.org/10.1155/2022/9410266

Lepodise, L. M., Phiri, O. H. E., & Pheko-Ofitlhile, T. (2024). Characterization of bone and dung biochars for potential use as precursors for artificial fertilizers. *Spectroscopy Letters*, *57*(6), 342–348. https://doi.org/10.1080/00387010.2024.2353725

Li, D., Su, P., Tang, M., & Zhang, G. (2023). Biochar alters the persistence of PAHs in soils by affecting soil physicochemical properties and microbial diversity: A meta-analysis. *Ecotoxicology and Environmental Safety*, *266*, 115589–115589. https://doi.org/10.1016/j.ecoenv.2023.115589

Li, H., Ishak, A. R., Mohd Aris, M. S., Mohamad Shaifuddin, S. N., Ding, S., & Deng, T. (2025). Enhanced Removal of Hexavalent Chromium from Water by Nitrogen-Doped Wheat Straw Biochar Loaded with Nanoscale Zero-Valent Iron: Adsorption Characteristics and Mechanisms. *Processes*, *13*(6), 1714. https://doi.org/10.3390/pr13061714

Li, J., Zheng, L., Wang, S.-L., Wu, Z., Wu, W., Nabeel Khan Niazi, Shaheen, S. M., Jörg Rinklebe, Bolan, N., Kim, K.-H., & Wang, H. (2019). Sorption mechanisms of lead on silicon-rich biochar in aqueous solution: Spectroscopic investigation. *Science of the Total Environment*, *672*, 572–582. https://doi.org/10.1016/j.scitotenv.2019.04.003

Li, Y., Wang, M., Shan, Y., Liu, J., Han, L., & Liu, X. (2024). Adsorption characteristics and molecular mechanisms of ionic organic pollutants on bone char. *Journal of Molecular Liquids*, *400*, 124624. https://doi.org/10.1016/j.molliq.2024.124624

Liang, M., Lu, L., He, H., Li, J., Zhu, Z., & Zhu, Y. (2021). Applications of biochar and modified biochar in heavy metal contaminated soil: A descriptive review. *Sustainability*, 13(24), 14041. https://doi.org/10.3390/su132414041

Liu, X., Xu, X., Dong, X., & Park, J. (2019). Adsorption characteristics of cadmium ions

from aqueous solution onto pine sawdust biomass and biochar. *BioResources*, *14*(2), 4270–4283. https://doi.org/10.15376/biores.14.2.4270-4283

Long, X.-X., Yu, Z.-N., Liu, S.-W., Gao, T., & Qiu, R.-L. (2024). A systematic review of biochar aging and the potential eco-environmental risk in heavy metal contaminated soil. *Journal of Hazardous Materials*, 472, 134345. https://doi.org/10.1016/j.jhazmat.2024.134345

Meng, F., Wang, Y., & Wei, Y. (2025). Advancements in Biochar for Soil Remediation of Heavy Metals and/or Organic Pollutants. *Materials*, *18*(7), 1524. https://doi.org/10.3390/ma18071524

Nazir, M. M., Li, G., Nawaz, M., Hameed, R., Zulfiqar, F., Jalil, S., Li, J., Zheng, X., Zhao, X., & Du, D. (2025). Biochar ameliorates heavy metals and polycyclic aromatic hydrocarbons in the soil-plant interface. *Ecotoxicology and Environmental Safety*, *307*, 119346. https://doi.org/10.1016/j.ecoenv.2025.119346

Ogoko, E. C., Kelle, H. I., Akintola, O. & Eddy, N. O. (2023). Experimental and theoretical investigation of *Crassostrea* gigas (gigas) shells based CaO nanoparticles as a photocatalyst for the degradation of bromocresol green dye (BCGD) in an aqueous solution. *Biomass Conversion and Biorefinery*. https://doi.org/10.1007/s13399-023-03742-8.

Okorodudu, E. O., Ibe, K.A., Wisdom, I., & Akpeji, B.H. (2026). Isotherm evaluation and performance assessment of bone biochar at varied dosages for simultaneous removal of PAHs and heavy metals. *Communication in Physical Sciences (CPS),* 13(2), 380-402, https://dx.doi.org/10.4314/cps.v13i3.4

Phiri, Z., Moja, N. T., Nkambule, T. T. I., & de Kock, L.-A. (2024). Utilization of biochar for remediation of heavy metals in aqueous environments: A review and bibliometric analysis. *Heliyon*, 10(4), e25785. https://doi.org/10.1016/j.heliyon.2024.e25785

Piccirillo, C. (2023). Preparation, characterisation and applications of bone char, a food waste-derived sustainable material: A review. *Journal of Environmental Management*, *339*, 117896–117896. https://doi.org/10.1016/j.jenvman.2023.117896

Qiu, M., Liu, L., Ling, Q., Cai, Y., Yu, S., Wang, S., Fu, D., Hu, B., & Wang, X. (2022). Biochar for the removal of contaminants from soil and water: A review. *Biochar*, 4, 19. https://doi.org/10.1007/s42773-022-00146-1

Rashed, M. N., Gad, E., & Fathy, N. M. (2024). Efficiency of chemically activated raw and calcined waste fish bone for adsorption of Cd (II) and Pb (II) from polluted water. *Biomass Conversion and Biorefinery*. *14*, 31703-31720. https://doi.org/10.1007/s13399-023-04885-4

Sharma, S., Bolan, N., Mukherjee, S., *et al*. (2025). Role of organic and biochar amendments on enhanced bioremediation of soils contaminated with persistent organic pollutants (POPs). *Current Pollution Reports*, *11*, 33. https://doi.org/10.1007/s40726-025-00361-x

Singh, R. K., & Singh, S. K. (2025). Persistent polycyclic aromatic hydrocarbons (PAHs) in the soil, its bioremediation, and health effects. *Environmental Sciences Europe*, *37*(1). https://doi.org/10.1186/s12302-025-01230-6

Wang, L., Yang, J., Li, X., Zhang, L., Van Zwieten, L., Mašek, O., Joseph, S., Zhang, K., & Yu, K. (2026). Engineered biochar composite with minerals: organo-mineral interactions, physicochemical changes, and implications for practical application.

Biochar, *8*(1). https://doi.org/10.1007/s42773-026-00569-0

Weber, W. J., & Morris, J. C. (1963). Kinetics of Adsorption on Carbon from Solution. *Journal of the Sanitary Engineering Division*, *89*(2), 31–59. https://doi.org/10.1061/jsedai.0000430

Wei, Z., Wei, Y., Liu, Y., Niu, S., Xu, Y., Park, J.-H., & Wang, J. J. (2024). Biochar-based materials as remediation strategy in petroleum hydrocarbon-contaminated soil and water: Performances, mechanisms, and environmental impact. *Journal of Environmental Sciences*, *138*(16), 350–372. https://doi.org/10.1016/j.jes.2023.04.008

Wei, Z., Wei, Y., Liu, Y., Niu, S., Xu, Y., Park, J.-H., & Wang, J. J. (2024). Biochar-based materials as remediation strategy in petroleum hydrocarbon-contaminated soil and water: Performances, mechanisms, and environmental impact. *Journal of Environmental Sciences*, *138*(16), 350–372. https://doi.org/10.1016/j.jes.2023.04.008

Wongcharee, S., Kandasamy, B., Govindasamy, P., Tansomros, P., Hongthong, S., Sangsida, W., Phibanchon, S., Chotigawin, R., Pahasup-anan, T., Pannaracha, P., Nakyai, T., & Suwannahong, K. (2025). Pig bone-derived biochar from food industry waste for heavy metal remediation: Sustainable consumption and production. *Results in Engineering*, *28*, 108003. https://doi.org/10.1016/j.rineng.2025.108003

Yaseen, Z. M., & Alhalimi, F. L. (2025). Heavy metal adsorption efficiency prediction using biochar properties: a comparative analysis for ensemble machine learning models. *Scientific Reports*, *15*, Article 13434. https://doi.org/10.1038/s41598-025-96271-5

Zhang, J., Wu, J., Yang, Z., & Xu, Z. (2020). Adsorption of polycyclic aromatic hydrocarbons by biochars: Sorption mechanisms and influencing factors. *Environmental Research*, 183, 109183. https://doi.org/10.1016/j.envres.2020.109183.

Zhao, J., Shen, X.-J., Domene, X., Alcañiz, J.-M., Liao, X., & Palet, C. (2019). Comparison of biochars derived from different types of feedstocks and their potential for heavy metal removal in multiple-metal solutions. *Scientific Reports*, *9*(1). https://doi.org/10.1038/s41598-019-46234-4

Dong, Y., Guan, X., & Lin, H. (2026). Biochar for simultaneous soil remediation and carbon sequestration: Application, mechanism, and development prospect – A comprehensive review. *Environmental Earth Sciences, 85*, Article 98. https://doi.org/10.1007/s12665-026-12834-3

Gao, X., Jia, R., Zhang, Y., Kang, J., Zhang, L., Ye, H., & Ren, H. (2026). Biochar for the adsorption of endocrine-disrupting chemicals: Performance, mechanisms, and strategies. *RSC Advances, 16*(12), 10310–10335. https://doi.org/10.1039/D5RA08986G

Laishram, D., Kim, S.-B., Lee, S.-Y., & Park, S.-J. (2025). Advancements in biochar as a sustainable adsorbent for water pollution mitigation. *Advanced Science, 12*(19), Article e2410383. https://doi.org/10.1002/advs.202410383

Li, P., Liu, Y., Sun, Y., & Zhang, C. (2026). Biochar innovations for organic pollutant remediation in contaminated soils. *Molecules, 31*(3), Article 432. https://doi.org/10.3390/molecules31030432

Mogashane, T. M., Motlatle, M. A., Mkhohlakali, A. C., Mokoena, L. V., & Tshilongo, J. (2026). Biochar-based adsorption of polycyclic aromatic hydrocarbons in contaminated soils: Advances, mechanisms, and bibliometric analysis. *Results in Engineering, 30*, Article

110374. https://doi.org/10.1016/j.rineng.2026.110374

Onmonya, Y. A., Adamu, S. G., & Sadiq, M. (2022). Potential of biochar for clean-up of heavy metal contaminated soil and water. *African Journal of Environmental Science and Technology, 16*(4), 146–154. https://doi.org/10.5897/AJEST2021.3038

Viotti, P., Marzeddu, S., Antonucci, A., Décima, M. A., Lovascio, P., Tatti, F., & Boni, M. R. (2024). Biochar as alternative material for heavy metal adsorption from groundwaters: Lab-scale (column) experiment review. *Materials, 17*(4), 809. https://doi.org/10.3390/ma17040809

Wang, T., Su, D., Wang, X., & He, Z. (2020). Adsorption-degradation of polycyclic aromatic hydrocarbons in soil by immobilized mixed bacteria and its effect on microbial communities. *Journal of Agricultural and Food Chemistry, 68*(50), 14907–14916. https://doi.org/10.1021/acs.jafc.0c04752

Zhang, W., Zhang, Z., & Diao, Z. (2026). Remediation of heavy metals and organic pollutants in soil by biochar: A comprehensive review. *C, 12*(2), 42. https://doi.org/10.3390/c12020042

Zhou, X., Chen, M., Wu, S., Zhou, X., Li, L., & Ma, Z. (2024). Heavy metals and PAHs adsorption characteristics of bio-asphalt in road runoff. *Journal of Cleaner Production, 450*, Article 141923. https://doi.org/10.1016/j.jclepro.2024.141923

Consent for publication

Not Applicable

Availability of data and materials

The publisher has the right to make the data public

Competing interests

The authors declared no conflict of interest. The study was conducted collaboratively with contributions
from all authors.

Funding

There was no source of external funding.

Author's Contribution

Kenneth A. Ibe, Wisdom Ivwurie participated in conceptualization, methodology, validation and supervision while, Emmanuel O. Okorodudu and Bamidele H. Akpeji performed the investigation, sample collection and preparation, data curation and formal analysis.